FOURTEENTH EUROPEAN ROTORCRAFT FORUM

Paper No. 70

INFLUENCE OF GROUND EFFECT ON HELICOPTER TAKEOFF AND LANDING PERFORMANCE

T. Cerbe - G. Reichert
TECHNISCHE UNIVERSITÄT BRAUNSCHWEIG, FRG
H.C. Curtiss Jr.
PRINCETON UNIVERSITY, USA

20. - 23. September, 1988
MILANO, ITALY

ASSOCIAZIONE INDUSTRIE AEROSPAZIALI
ASSOCIAZIONE ITALIANA DI AERONAUTICA ED ASTRONAUTICA

INFLUENCE OF GROUND EFFECT ON HELICOPTER TAKEOFF AND LANDING PERFORMANCE

T. Cerbe - G. Reichert
TECHNISCHE UNIVERSITÄT BRAUNSCHWEIG, FRG
H.C. Curtiss Jr.
PRINCETON UNIVERSITY, USA

Abstract

The calculation of helicopter takeoff and landing performance demands a high accuracy in determining power required. Power required is significantly influenced by ground effect depending on distance of the helicopter rotor above ground and on forward velocity. Ground effect changes the induced velocity of the rotor and thereby the induced power. For hover, the ground effect produces at constant power an increased thrust with decreasing distance of the helicopter from the ground. For constant thrust, power required will be reduced. At low forward speeds the influence of ground effect decreases rapidly with increasing velocity. This can be mainly explained by the recirculation, which occurs for low forward velocity in front of the rotor. With increasing velocity a ground vortex forms under the rotor.

Recent research deals with the experimental determination of the recirculation effect as well as the strength and the position of the ground vortex. Also there exist some theoretical approaches describing the influence of the ground vortex. However, these present approaches do not provide sufficient accuracy to calculate power required in ground effect at low forward velocity. Especially during takeoff of the helicopter without power excess, the recirculation and the ground vortex have a considerable influence on the practicable flight path. While out of ground effect, power required decreases with increasing forward velocity proceeding from hover, in ground effect power required increases due to the recirculation. In addition, low horizontal accelerations influence the recirculation and the ground vortex state.

The influence of ground effect on power required for hover and forward flight will be shown by experimental results from flight tests with a BO 105 helicopter as well as from track tests with a model rotor. Theoretical performance calculations will be compared with experimental results and discussed. In the performance calculation a semi-empirical model for the ground effect is used. The performance calculation and the simulation model for simulation of takeoff and landing procedures will be described. The influence of ground effect on helicopter flight path will be discussed by means of simulation results.

Notation

a	blade lift curve slope	
a_x	horizontal acceleration	
$\bar{a}_x$	non-dimensional horizontal acceleration	$\bar{a}_x=a_xR/w_iH^2$
A_i	polynomial coefficient	
b	blade chord	
C_Q	torque coefficient,	$C_Q=Q/\rho U^2RS$
C_{Qi}	coefficient for induced torque	
C_T	thrust coefficient,	$C_T=T/\rho U^2S$
H	rotor height above ground	
$\bar{H}$	non-dimensional height,	$\bar{H}=H/R$
H_{SKID}	skid height	
K	constant	
K_G	weight coefficient,	$K_G=2G/\rho U^2S$
K_P	power coefficient,	$K_P=2P/\rho U^3S$
K_{PH}	power coefficient in hover	
K_{Po}	coefficient for profile power	
P_i	induced power	
P_{iH}	induced power in hover	
P_{req}	power required	
Q	torque	
Q_S	source strength	
R	rotor radius	
S	disc area	
t	time	
T	thrust	
T_L	time constant	
$\bar{T}_L$	non-dimensional time constant,	$\bar{T}_L=T_Lw_iH/R$
u_{Kg}	horizontal velocity in geodetical coordinate system	
$\bar{u}_{Kg}$	non-dimensional horizontal velocity,	$\bar{u}_{Kg}=u_{Kg}/w_iH$
$\dot{u}_{Kg}$	horizontal acceleration	
$\bar{\dot{u}}_{Kg}$	non-dimensional horizontal acceleration,	$\bar{\dot{u}}_{Kg}=\dot{u}_{Kg}R/w_iH^2$
U	rotor tip speed	
V	horizontal speed	
$\bar{V}$	non-dimensional horizontal speed,	$\bar{V}=V/w_iH$
w_i	average induced velocity at the rotor disc	
$\bar{w}_i$	non-dimensional induced velocity,	$\bar{w}_i=w_i/U$

w_{iH}	induced velocity in hover	
w_{Kg}	vertical velocity	
$\bar{w}_{Kg}$	non-dimensional vertical velocity,	$\bar{w}_{Kg}=w_{Kg}/w_{iH}$
x	takeoff distance	
X_{GV}	factor for ground vortex influence	
X_{SM}	factor from source model	
X_P	power factor	
z	number of blades	
α_{Ro}	shaft angle of attack	
δ	profile drag coefficient	
Θ	longitudinal pitch	
$\Theta_{0.75R}$	collective pitch at three quarters radius	
Ω	rotor speed	
ρ	air density	
σ	solidity	$\sigma=zb/\pi R$
DFG	Deutsche Forschungs Gemeinschaft	
DFVLR	Deutsche Forschungs- und Versuchsanstalt für Luft- und Raumfahrt e.V.	
IGE	in ground effect	
OGE	out ground effect	
SFB	Sonderforschungsbereich	

BO 105 Rotor Data	Model Rotor Data
R = 4.91 m	R = 1.22 m
b = 0.27 m	b = 0.06 m
z = 4	z = 4
Ω = 44.4	Ω = 47.25
σ = 0.07	σ = 0.066
Twist: 8°	Twist: 8°

1. Introduction

The simulation of takeoff and landing trajectories requires a high accuracy in the calculation of power required and power available, since the resulting power excess determines the flight path. This paper is focussed on determination of power required, assuming that power available is known from manufacturer engine data fields. Power required depends on helicopter gross weight, atmospheric conditions, flight state, i.e. longitudinal accelerations and velocities, and ground proximity of the helicopter. For low skid heights, the ground influences the aerodynamics and flightmechanics of the helicopter. The so-called ground effect for hover has been well known since the beginning of helicopter development. The first helicopters had only the capability to hover IGE (In Ground Effect). However, the favourable ground effect, a decrease of power required with decreasing skid height, is rapidly reduced with increasing horizontal velocity. The influence of skid height and horizontal velocity has been investigated experimentally as well as theoretically.

Regarding the takeoff without power excess, the ground effect influence is of great importance. Takeoff without power excess is performed with constant hover power IGE, since no additional power is available. This takeoff results in considerable height loss accelerating from hover. The height loss is significantly influenced by the ground effect. Whether a takeoff is possible or not depends on the takeoff power available, the skid height in hover, the increase of power required with increasing velocity and the acceleration. Also without ground effect the height loss depends on the acceleration due to required forward tilt of the rotor. Increasing height loss is obtained with increasing acceleration OGE (Out Ground Effect). Recent experimental ground effect investigations with a model rotor show that low horizontal accelerations and also decelerations significantly influence the ground effect. For the simulation of takeoff without power excess this dynamic ground effect has to be taken into account.

In the following the steady state ground effect for hover and forward flight is discussed by means of experimental results from flight test with a BO 105 helicopter. The experimental results are compared with theoretical results from performance calculations. A modified source model is used to describe the ground effect. The dynamic ground effect for low forward velocities, the influence of acceleration and deceleration, respectively, is discussed by means of experimental results from model rotor tests carried out in a special track facility at Princeton University. Taking the stationary and the dynamic ground effect into account, the takeoff without power excess is investigated theoretically. A quasi-stationary data field simulation model is used. The simulation results are verified by flight test results. Finally the simulation of a vertical landing with constant power setting is carried out.

2. Steady State Ground Effect in Hover

The first experimental investigations dealing with a helicopter rotor hovering IGE (In Ground Effect) had been carried out by KÜSSNER /1/ in 1937. At the same time, BETZ /2/ tried to describe the ground effect for hover by an analytical approach. They found that the ground effect mainly influences the induced power part of the total power required by changing the induced velocity at the rotor disc. The analytical approach of Betz used the method of mirror images, where the rotor is replaced by an aerodynamic model. This way, the boundary condition at the ground plane of vertical velocity equal to zero is satisfied. The method of mirror images is used in all analytical approaches, e.g. /3-6/.

Figures 1 and 2 show the helicopter hovering out and in ground effect. For hover OGE the air particles, accelerated by the rotor, form a contracted free rotor wake, while for hover IGE, the rotor wake is restricted by the ground. The aerodynamics of the helicopter in hover IGE is quite complex, also

due to the different interference effects between rotor, fuselage, ground and tailrotor. Therefore any analytical approach can be only an approximation to real physics of ground effect.

A relatively simple model is the source model of CHEESEMAN and BENNETT /4/, which has been the first model that includes the influence of forward velocity on power required IGE. Figure 3 shows the source model for hover and forward flight IGE. The mirror rotor is replaced by a source with the strength QS. The source induces an additional velocity at the rotor disc leading to a decreasing total inflow velocity at the rotor. For the condition of constant rotor thrust, the relation of the induced velocities for hover ($V=0, \Theta=0$) IGE and OGE can be expressed as a function of the non-dimensional height $\bar{H}=H/R$:

$$\left[\frac{w_{iH,IGE}}{w_{iH,OGE}}\right]_{T=const} = \left[1 - \frac{1}{16}\cdot\left[\frac{1}{\bar{H}}\right]^2\right]^{3/2} \tag{1}$$

The momentum theory gives for constant thrust the following relationship for the induced power in hover IGE and OGE:

$$\left[\frac{P_{iH,IGE}}{P_{iH,OGE}}\right]_{T=const} = \left[\frac{w_{iH,IGE}}{w_{iH,OGE}}\right]_{T=const} \tag{2}$$

The source model shows reasonable agreement with flight test results for the hover case at certain rotor heights above ground, relevant for most helicopters. Therefore, this model has been chosen for the investigations carried out here.

An evaluation of flight test data from several helicopters for hover IGE has been made by HAYDEN /7/. He has found an empirical relationship for the power factor IGE and OGE of the form:

$$\frac{K_{IGE}}{K_{OGE}} = \frac{1}{0.9926 + 0.15176\left[\frac{1}{\bar{H}}\right]^2} \tag{3}$$

This relation is based on the assumption that the part of total power required, which depends on the thrust, the helicopter weight, respectively, is influenced by the ground effect. The power coefficient for hover OGE can be written as:

$$K_{PH} = K_{PO}\,(K_G=0) + K_{OGE}\cdot K_G^{3/2} \tag{4}$$

The power coefficient for hover IGE is then:

$$K_{PH,IGE} = K_{PO}\,(K_G=0) + K_{IGE}\cdot K_G^{3/2} \tag{5}$$

The power factor of HAYDEN can be used for comparison with flight tests or with theoretical results.

A further step to describe power required for hover OGE has been taken by LIESE, RUSSOW and REICHERT /8/. The result of their approach is a power coefficient of the form:

$$K_{PH,OGE} = K_{PO}\,(K_G=0) + \Delta K_{PH,OGE}\,(K_G) \tag{6}$$

with:

$$\Delta K_{PH,OGE} = A_1\cdot K_G + A_2\cdot K_G^2 + \ldots \tag{7}$$

By means of a regression analysis of BO 105 flight test data for hover OGE they found that a second order polynomial gives the best agreement with flight tests.

The ground effect is usually expressed relative to power required OGE, or the induced power OGE, respectively. Therefore, the knowledge of power required OGE is of great importance. Figure 4 shows the power coefficient versus weight coefficient from hover tests OGE with a BO 105. Analogous to

HAYDEN, the power coefficient for hover IGE can be written as:

$$K_{PH,IGE} = K_{PO}\,(K_G=0) + XP_{IGE}\cdot\Delta K_{PH,OGE}\,(K_G) \qquad (8)$$

Extensive hover flight tests IGE up to a skid height of 100ft have been carried out with the BO 105 helicopter of the DFVLR. For the analysis of the data from these flight tests the following equation has been used:

$$XP_{IGE} = \frac{K_{PH,IGE} - K_{PO}}{\Delta K_{PH,OGE}} = \frac{\Delta K_{PH,IGE}}{\Delta K_{PH,OGE}} \qquad (9)$$

Figure 5 shows the power factor IGE versus the non-dimensional rotor height above ground and the skid height, respectively. In the region of $\bar{H}$=0.6-1.7 the flight test data agree well with the classical ground effect theory. The performance calculation with the source model and also the empirical relationship of HAYDEN show very good agreement with the regression curve of the flight tests. Only the vortex model (triangular disc load distribution, a_{R0}=0) from HEYSON /9/ overpredicts the ground effect. Non-dimensional heights in the region of $\bar{H}$=0.8-1.2 are relevant for takeoff of the BO 105 (HSKID≈3-10ft).

From the height $\bar{H}$=1.7 up to the height $\bar{H}$=4.0 the power factor XP is greater than 1.0, consequently power required IGE is greater than power required OGE. The increase of power required is about 3% of the induced power $\Delta K_{PH,OGE}$. Classical ground effect theory gives that for heights $\bar{H} \geq 2.0$ the ground effect can be neglected. Owing to this, most experimental ground effect investigations have examined hover heights up to $\bar{H}$=2.0. If one would take the flight test data between $\bar{H}$=2.0 and $\bar{H}$=3.0 from Figure 5 as data OGE, one would get a regression curve similar to the empirical relation of HAYDEN.

A regression analysis of the BO 105 flight test data for hover IGE as well as for hover OGE has been made by CERBE and RUSSOW /10/. They found that the power required in the region of $\bar{H} \geq 5.0$, Figure 5, agree with the power required OGE, Figure 4, so that in fact, there is a maximum power required at a certain height IGE. It is well known that flight tests IGE are very sensitive to low wind velocities. During these tests, the wind velocity has been recorded by wind measuring equipment up to heights of 50ft and has been less than 1m/s in any case. A regression analysis of the collective pitch IGE in /10/ shows the same trend as the power factor. The maximum collective pitch is required at a certain height IGE.

To demonstrate this power variation another way one can perform a simple flight test. The test starts at a height of about $\bar{H}$=10 with a vertical descent velocity of 1m/s≈200ft/min. The pilot has to set the collective pitch required for steady descent. At a height of $\bar{H}$≈4.0 the helicopter first accelerates to a higher vertical velocity until the favourable ground effect increases, and the helicopter decelerates to hover IGE. Of course, the wind velocity should be less than 1m/s and the tests should be performed only by test pilots. Flight tests with the BO 105 have shown this effect described here.

To explain this variation one has to consider the superposition of two influences: The favourable effect, which decreases power required IGE with decreasing height is the so-called ground cushion effect. This effect can be described by the method of mirror images, e.g. the source model. The unfavourable effect, which increases power required, could be due to recirculation for hover IGE. Recirculation occurs for example for hover testing of model rotors in closed rooms, Figure 6.

The experimental investigations of KÜSSNER /1/,/11/, who has performed hover tests IGE with different model rotors in a closed room show the same trend as the BO 105 flight test data. Up to now, a recirculation for free hover flight tests IGE analogous to Figure 6 has not been observed. But it should be borne in mind that there is also a considerable upstream flow in the center of the rotor hovering IGE, Figure 7. This is well known and has been examined for example by JACKSON and HOUSE /12/, regarding exhaust gas reingestion during hover IGE. The reingestion is caused by a recirculation of the rotor downwash along the centerline of the rotor. This recirculation influences power available of the engines as well as power required. Investigations dealing with the quantitative determination of the inner recirculation are not known.

This experimental result that the power IGE exceeds the power required OGE may be critical in special cases for heavily loaded helicopters, operating with low power excess. Rescue operations close to the ground could be critical under extreme conditions. For takeoff, the effect is of less importance since normally the takeoff heights are considerably below the critical height of about $\bar{H}$=1.7. Independent of this, the effect should be kept in mind for hover flight testing IGE and OGE.

3. Steady State Ground Effect in Forward Flight

In forward flight the favourable ground effect decreases rapidly with increasing velocity, increasing wind velocity, respectively. Pilots know that at low heights and low velocities the helicopter tends to descent to the ground if forward velocity is developed while still maintaining hover power, hover collective pitch, respectively. CHEESEMAN and BENNETT /4/ have found from flight test IGE the strong increase in power required with low forward velocities and tried to describe the effect by the source model. However, the simple source model underestimates the ground effect in forward flight.

Some years later HEYSON /5/ extended the vortex cylinder model of KNIGHT and HEFNER /3/ to a skewed vortex cylinder for forward flight IGE. Further work by HEYSON resulted in different vortex models,

see for example /9/. These models do not include the ground vortex, which has been recognized from windtunnel tests as an important element of the flow field IGE, /13-15/. Independent of this, the vortex model of HEYSON seems to give reliable results for the increase in power required IGE with forward velocities. A comparison with windtunnel results of SHERIDAN /15/ is given by HEYSON /16/. Unfortunately, the models overpredict the ground effect in hover, see Figure 5.

CURTISS /17/ was the first to conduct ground effect investigations at low forward velocities with a model rotor in a special tracking facility. Contrary to windtunnel testing, where the air moves relative to the ground, this facility makes it possible to move the model through still air, simulating the forward flight IGE under realistic ground boundary conditions. Windtunnel tests IGE can be considered to represent the hover IGE under wind conditions, which do not necessarily give the same flow field as in forward flight IGE with zero wind, due to different ground boundary layers. CURTISS has found, that there exist two different flow regions, a large recirculation pattern in front of the rotor for very low velocities and a well defined ground vortex under the rotor with increasing velocity. Figures 8 and 9 show the recirculation and the ground vortex for forward flight IGE. Figure 10 shows the horseshoe vortex pattern. The recirculating flow induces in front of the rotor disc an additional downward velocity, which increases induced power, power required, respectively. This way, power required IGE is increased, exceeding power required for hover IGE at the same height with increasing low velocities. As the velocity is further increased, a ground vortex forms under the rotor inducing an upflow in front of the rotor disc. As a result power required is reduced. The recirculation is no longer existent when the ground vortex is set up. The ground vortex moves with increasing velocity backwards until it disappears behind the helicopter.

Some theoretical studies have taken into account the ground vortex. SUN /6/ used a theoretical approach based on experimental data to investigate the interaction of the rotor wake and the ground vortex for forward flight IGE. An analytical model for the ground vortex strength and position, has been developed by HE and GAO /18/. They used a free wake model in connection with the analytical ground vortex model and compared their results with experimental data from /6/. The advantage of the theoretical approaches based on physical assumptions is that they give aside from the experimental investigations additional insight into the physics of a phenomen. However, at present there does not exist an analytical model which describes the recirculation region or the ground vortex region with sufficient accuracy. Especially when a high accuracy is required, semi-empirical models often give the better results because they can easily be adjusted to match experimental data. A further advantage of these models is that they need in general less computation time. This is an important consideration in the simulation of helicopter takeoff and landing carried out in this paper. The model used here is a modified source model. The original source model for forward flight IGE has the form:

$$\left[\frac{w_{i,IGE}}{w_{i,OGE}}\right]_{T=const} = \left[1 - \frac{1}{16}\cdot\left[\frac{1}{\bar{H}}\right]^2 \cdot \frac{1}{1+\left[\frac{\bar{V}}{\bar{w}_{i,OGE}}\right]^2}\right]^{3/2} \tag{10}$$

Using the momentum theory for $\alpha_{R0}=0$ the relationship for the induced velocities can be written as a function of the non-dimensional forward velocity $\bar{V}=V/w_{iH,OGE}$:

$$\left[\frac{w_{i,IGE}}{w_{i,OGE}}\right]_{T=const} = \left[1 - \frac{1}{16}\cdot\left[\frac{1}{\bar{H}}\right]^2 \left[-\frac{1}{2}\bar{V}^2 + \sqrt{\frac{1}{4}\cdot\bar{V}^4 + 1}^{\,2}\right]\right]^{3/2} \tag{11}$$

Analogous to equation (2) one gets:

$$\left[\frac{P_{i,IGE}}{P_{i,OGE}}\right]_{T=const} = \left[\frac{w_{i,IGE}}{w_{i,OGE}}\right]_{T=const} \tag{12}$$

Equation (11) can be used to calculate the rotor inflow. The source model for forward flight IGE has been integrated into rotor calculation of a complex helicopter simulation program by CERBE and REICHERT /19/. The modification of the source model, accounting the recirculation/ground vortex influence, is described later.

It has been already mentioned that the knowledge of hover power required OGE is an essential precondition for determining the power factor IGE for hover, Figure 5. This is also valid for the calculation of the power factor for forward flight OGE as well as IGE. The data reduction method from /8/ which is used here, requires the hover power required as a basic reference. The power factor in general form is:

$$XP = \frac{K_P - K_{P0}}{\Delta K_{PH}} \tag{13}$$

The power factor has the value XP=1 for hover OGE.

The knowledge of power required in forward flight OGE is not essential for the data reduction IGE but is very helpful for comparison. Flight tests with the BO 105 have been carried out and are described in /8/. Figure 11 shows the power factor in forward flight OGE as a function of non-dimensional forward velocity. The trimmed power required from the performance calculation, from the simulation program /19/, respectively, agrees well with the regression curve of the BO 105 flight test data. The differences are in the range of ±3% of the induced power in hover.

Figures 12 and 13 show the power factor in forward flight IGE from BO 105 flight tests versus non-dimensional velocity. Flight tests have been performed under wind conditions with wind velocities less than 1m/s for low skid heights H_{SKID}=0.5-2.5m ($\bar{H}\approx 0.8$-1.0) which are primarily of interest for takeoff of the BO 105. In both figures, the regression curve OGE is shown for comparison. Regarding the flight test data IGE, an increase of power factor for low forward velocities can be clearly identified, which is explained previously by the recirculation state. With increasing velocity the large recirculation pattern, see also Figure 8, diminishes and a ground vortex arises under the rotor. It can be seen from Figures 12 and 13 that in the region of $\bar{V}$=0.7 the power factor reaches nearly the power factor OGE. For forward velocities $\bar{V}\approx 1.0$, there may be a small ground effect similar to ground effect of an airplane but this effect is less than the scatter of flight test data in forward flight OGE.

The performance calculation with the source model, which predicts very well the ground effect influence in hover, Figure 5, agrees also with the power factor in hover IGE, Figures 12 and 13. Differences occur in the recirculation/ground vortex region at forward velocities of $\bar{V}$=0.1-1.0. In this region, the source model has been modified in a way which is described in the following. The performance calculation with the modified source model shows good agreement with the flight test data IGE. The performance calculation OGE, Figure 11, is not shown again in these figures but it should be mentioned that the source model gives nearly no ground effect for forward velocities $\bar{V}\approx 1.5$. Owing to this, the calculated curves for $\bar{V}\geq 1.5$ represent nearly the OGE calculation.

Taking into account the influence of the recirculation, the ground vortex, respectively, the source model can be modified in different ways. Here, a mathematical description of the influence on the power factor is chosen, which can easily be adjusted to flight test results. Figure 14 shows the boundaries for recirculation and ground vortex flow regimes determined from flow visualization studies /17/. Assuming that in the middle of the recirculation regime, the influence of the recirculation reaches a maximum, a velocity $\bar{V}_m$ can be determined from this figure. As approximation, a linear function between $\bar{V}_m$ and the non-dimensional height $\bar{H}$ is used:

$$\begin{aligned} \bar{V}_m &= 0.72 - 0.206 \cdot \bar{H} \qquad (\bar{H} < 3.5) \\ \bar{V}_m &= 0.0 \qquad\qquad\qquad\qquad (\bar{H} \geq 3.5) \end{aligned} \tag{14}$$

This function gives for $\bar{H}\geq 3.5$ negative values of $\bar{V}_m$, so that equation (14) is valid for $\bar{H}<3.5$. For the variation of induced power due to the recirculation/ground vortex a simple parabola is used. The modified source model has the form:

$$\left[\frac{P_{i,IGE}}{P_{i,OGE}}\right]_{T=const.} = \left[1 - X_{SM} \cdot X_{GV}\right]^{3/2} \tag{15}$$

In this equation, factor X_{SM} gives the influence of the source model (the ground cushion effect) and factor X_{GV} gives the influence of the recirculation/ground vortex:

$$X_{SM} = \frac{1}{16}\cdot\left[\frac{1}{\bar{H}}\right]^2 \left[1 - \bar{V}^2 + \sqrt{\frac{1}{4}\cdot\bar{V}^4 + 1}\right]^2 \tag{16}$$

$$X_{GV} = 1 - 2\cdot X_{GV,max}\ \frac{\bar{V}}{\bar{V}_m} + X_{GV,max}\cdot\left[\frac{\bar{V}}{\bar{V}_m}\right]^2 \tag{17}$$

$$X_{GV} = 1 \qquad (\bar{V}_m = 0)$$

Factor $X_{GV,max}$ can be used to adjust the theory to match the flight test results. Reasonable agreement is obtained here for $X_{GV,max}$=0.5 in the region of low BO 105 skid heights H_{SKID}=0.5-2.5m (Figures 12 and 13). This means that the ground cushion effect is reduced to fifty percent of its value at a forward velocity $\bar{V}=\bar{V}_m$ (assuming that the source model describes the ground cushion effect).

It should be noted that the factor $X_{GV,max}$ may change for significantly lower heights, for other types of helicopters, respectively. Also, the boundary between the recirculation and ground vortex regions shown in Figure 14, and thus the function of $\bar{V}_m$, may be slightly influenced by the rotor-fuselage-ground interaction, differing from one helicopter ot another. However, for performance calculation and simulation of takeoff and landing, which are primarily of interest here, this simple model is of practical use.

4. Dynamic Ground Effect in Forward Flight

A number of studies of the ground effect on a lifting rotor have been conducted with a 2.44m diameter model rotor in a unique facility at Princeton University, the Princeton Dynamic Model Track. A cross section drawing of the facility and model is shown in Figure 15. Experimental investigations included two series of force and moment measurements, flow visualization studies and hot wire surveys of the flow field as reported in /20-23/ and /6/. Complete experimental data are presented in /22/, /23/ and /6/. In this paper, the results of an analysis of the thrust and torque measurements to estimate the induced power variation in ground effect are presented. Previous analysis of the data as in /3/ focussed on the determination of the harmonic inflow components. In this study the average inflow through the rotor is calculated and used to develop an estimate of the induced power as described below.

Two new results were obtained from these experimental investigations. First, flow visualization studies showed two distinct flow regimes IGE, corresponding to different wake distortion patterns. At the lower end of the advance ratio range investigated, there is a recirculating flow field where the rotor wake flows forward along the ground, is deflected upwards and then back down through the rotor as depicted by the sketch in Figure 8 and the photograph in Figure 16. The lateral flow components of this recirculating flow are small. At higher speeds, above a critical non-dimensional velocity, a well-defined vortex is formed under the rotor, aft of the rotor leading edge as shown in Figures 9 and 17. This vortex is roughly of horseshoe shape as shown in Figure 10. Its presence markedly distorts the leading edge of the wake. A semi-empirical theory has been developed by SUN /6/ for the ground vortex flow regime but no theory exists for the recirculation regime. SUN showed that the ground vortex is responsible for wake distortion and consequently a marked change in the inflow. As will be shown below these large distortions of the wake produce correspondingly large variations in the average rotor inflow compared to that which would be predicted by cylindrical wake models such as those of HEYSON /9/. The second important result of the experimental studies is the sensitivity of the rotor forces and moments to translational acceleration and deceleration, an aspect of the experiments that could be readily examined since a moving model facility was used. As described below, this acceleration sensitivity indicates that significant time constants are associated with the development of these flow fields.

The experimental data presented in /22/ and /23/ were analyzed to determine the average inflow through the rotor IGE which can be directly related to the variation of induced power IGE. There are three possible approaches to the determination of the average inflow. The blade element expression for thrust coefficient can be used:

$$\frac{C_T}{\sigma} = \frac{a}{6}\cdot\Theta_{.75R} - \frac{a}{4}\cdot\bar{w}_i \tag{18}$$

Given experimental measurements of the thrust, collective pitch and the rotor parameters, the average inflow $\bar{w}_i$ can be calculated. A second method is to use the blade element expression for the induced torque coefficient assuming that the inplane-force contribution is negligible as it would be at these low advance ratios:

$$\frac{C_{Qi}}{\sigma} = \left[\frac{a}{6}\cdot\Theta_{.75R} - \frac{a}{4}\cdot\bar{w}_i\right]\cdot\bar{w}_i \tag{19}$$

This approach is not satisfactory due to the fact that for typical operating conditions, the variation of C_{Qi} with $\bar{w}_i$ is very small and so the lack of sensitivity of this method makes it an undesirable approach. A third approach would be to use the torque equation in another form:

$$\frac{C_Q}{\sigma} = \frac{C_T}{\sigma}\cdot\bar{w}_i + \frac{\delta}{8} \tag{20}$$

Assuming that the profile drag coefficient δ is known measured values of C_Q and C_T can be used to determine $\bar{w}_i$. Equation (18) was used to determine the inflow in these investigations. Calculations were also made using equation (20) with an estimated drag coefficient. The results were consistent with those obtained from equation (18). This approach is similar to that of reference /24/. However, the uniform inflow values obtained in /24/ are inconsistent with the power measurements and therefore are not discussed here. The induced power is:

$$\frac{C_{Qi}}{\sigma} = \frac{C_T}{\sigma}\cdot\bar{w}_i \tag{21}$$

and the non-dimensional power factor becomes:

$$XP = \frac{\bar{w}_i}{\sqrt{\frac{C_T}{2}}} \tag{22}$$

Equations (21) and (22) strictly speaking, assume that the inflow velocity is constant over the rotor disc and so slightly different value of $\bar{w}_i$ could be obtained by the two different equations, i.e., equation (21) assumes that the induced power is given by simple momentum theory. Unfortunately insufficient model data were available to use the more sophisticated approach applied to the flight test data described in this paper to determine the hovering power factor and the experimental value of the profile power. Thus the factor XP may be overestimated. However, this approximation should not influence the shape of the curves.

Experimental data from the model tests at three non-dimensional heights are shown in Figures 18, 19, and 20. Figure 18 at the lowest height shows only steady state (i.e., constant translational velocity data) and serves to illustrate the importance of the two flow regimes influencing the shape of the inflow variation (normalized induced power), causing a significant departure from theory.

As the non-dimensional velocity is increased there is a significant increase in the downward inflow through the rotor due to the recirculation, corresponding to increasing XP. Roughly the inflow increases proportional to non-dimensional horizontal velocity up to a critical velocity. This additional downward flow is a result of the recirculating flow field and causes a significant rise in induced power with velocity. Above a critical non-dimensional velocity, the average inflow decreases rapidly with velocity. This is due to the formation of the ground vortex which distorts the leading edge of the rotor wake upward as shown in Figures /9/ and /17/ reducing the downward flow. The ground vortex only exists over a rather narrow speed range and above a non-dimensional velocity the inflow follows the OGE curve. These inflow variations determined by this analysis are supported by the hot wire measurements of the flow field under the rotor reported by SUN in /6/. At this low height, it was also noted that there was considerable sensitivity to acceleration with low level of acceleration ($\bar{a}_X$=0.013) producing a shift in the velocity at which the recirculation region disappears and the ground vortex flow forms.

The effect of longitudinal acceleration was examined in detail at $\bar{H}$=0.68 as shown in Figure 19. The induced power factor variation with non-dimensional velocity is shown for three levels of non-dimensional acceleration. At the lowest acceleration ($\bar{a}_X$=0.013) the characteristic shape shown by the steady state data at the lower height in Figure 18 is evident. For the two higher levels of acceleration ($\bar{a}_X$=0.063, 0.130) the peak in the power factor almost disappears indicating that there was insufficient time for the recirculation pattern to be established and consequently there is only a small increase in induced power. The effect of the ground vortex formation is still evident as a break in the curve corresponding to a relative reduction in inflow through the rotor disc. The dependence on acceleration indicates that a relatively long time constant or delay time is associated with the full development of the recirculation flow.

An approximate delay time can be associated with the effect of acceleration in this complex flow field. The variation of XP with acceleration shown in this figure indicates that a non-dimensional delay time of the order of $\bar{T}_L \approx 10.0$ is associated with the development of the recirculating flow field. This is a time scale similar to that associated with the wake flow traversing the circumference of circle of radius R ($\bar{T}_L = 2\pi$). Very low accelerations delay the build up of recirculation in such a way that the inflow occurs at a correspondingly higher velocity, while at the higher accelerations there is insufficient time for the recirculation to be set up and consequently a much smaller increase in the power factor is present. The effect of deceleration also follows this model as can be determined from the data in /22/.

Unfortunately only a small number of steady state data points at a non-dimensional height of $\bar{H}$=0.86 were taken, Figure 20. Hot wire measurements /6/ indicate that they are in the region where the ground vortex is formed, and thus the induced power decreases with velocity. Comparison of these three curves shows that the peak value of the power factor reduces with increasing non-dimensional height indicating a reduction in the strength of the recirculation and the ground vortex as height is increased.

5. Influence of Ground Effect on Takeoff and Landing

It has been shown in the previous sections that power required is significantly influenced by ground effect, depending on helicopter height above ground, forward velocity and horizontal acceleration. Since the takeoff and landing performance of helicopter is determined by power required and power available, ground effect has an important influence on takeoff and landing flight path. Investigations relating to the optimization of takeoff and landing by CERBE and REICHERT /25/ have shown that especially the flight path for takeoff without power excess is very sensitive to the ground effect. A takeoff without power excess has to be performed if power available equals hover power required IGE for low skid heights, i.e. the takeoff is carried out with constant collective pitch, constant hover power IGE, respectively. Whether a takeoff without ground contact is possible or not depends mainly on the horizontal acceleration. In the following, this critical takeoff procedure will be considered in more detail.

For simulation of takeoff and landing the quasi-stationary data field simulation model from /19/ is used. This simulation model contains the longitudinal motion of the helicopter, assuming quasi-stationary pitching motion. Angular velocities and accelerations have a negligible influence on power required, thus they are not considered in the model. Figure 21 shows a typical data field OGE in non-dimensional form. The data fields contain the power factor XP as a function of the non-dimensional

horizontal and vertical velocities $\bar{u}_{Kg}$, $\bar{w}_{Kg}$ and ground effect height $\bar{H}$. For different values $\bar{H}$, different levels in the diagram are obtained. In addition to the forward flight diagram the power coefficient for hover, as a function of the weight coefficient, is required.

Takeoff and landing are characterized by translational accelerated flight states. Because the data fields contain only stationary states, the accelerated states are transformed into equivalent stationary states, e.g. a horizontally accelerated forward flight becomes an equivalent stationary climb with an equivalent gross weight. Both flight states have similar inflow angle, control input and power required. A more detailed description of the development of data field simulation is given in /19/. The data reduction methods can be found in /8/,/10/.

The height loss during takeoff with constant power is of primary interest. In the case of takeoff OGE, the height loss results from the forward tilt of the rotor thrust required for horizontal acceleration. With increasing forward velocity, and thus decreasing induced power, an additional "power excess" can be used for horizontal acceleration or climb. The height loss depends mainly on horizontal acceleration and on horizontal velocity. Figure 22 shows the influence of horizontal acceleration on height loss for takeoff with constant hover power OGE.

The figure shows that higher horizontal acceleration, i.e. higher forward tilt of rotor thrust, leads to a greater height loss. For the lower accelerations only a small height loss occurs. This can be explained by the relatively strong decrease in induced power with increasing forward velocity. The height loss depends on the gradient of induced power $dXP/d\bar{V}$ near hover, see for example Figure 11. Considering the low acceleration case, the helicopter starts to climb before the horizontal acceleration is reduced. This is not the case for the acceleration of $\dot{u}_{Kg}=3m/s^2$ where the climb begins with decreasing horizontal acceleration. Higher accelerations result in shorter horizontal takeoff distances, which are not shown here.

Figure 23 shows the influence of horizontal velocity on height loss for takeoff with constant power OGE for the higher acceleration.

For this acceleration the climb begins with a decrease in horizontal acceleration, and thus increasing forward velocity leads to increasing height loss. It should be noted that forward velocities reached during the acceleration maneuver are lower than the forward velocity for minimum power required, the velocity for maximum climb velocity, respectively. For the BO 105 the velocity for minimum power required is $V_y \approx 28m/s$. Acceleration to velocities higher than this velocity would result in a considerably higher height loss. For takeoff, velocities below or equal V_y are of practical interest. A typical forward velocity for the BO 105 reached during acceleration IGE is in the order of $u_{Kg}=15m/s \approx 30kts$.
Figures 24 and 25 show a takeoff with constant power IGE for two skid heights ($\bar{H}=1.0$, $H_{SKID}=2.0m$ and $\bar{H}=0.8$, $H_{SKID}=1.0m$) and the three acceleration maneuvers from Figure 22. Simulation with the source model gives nearly no height loss for the lowest acceleration. The source model does not include the influence of the recirculation, the ground vortex, respectively, thus there is no increase of power required with forward velocity. The gradient of the power curve IGE near hover is similar to the gradient OGE. The height loss for higher accelerations is slightly greater in comparison to the height loss OGE.

In contrast to this, simulation with the modified source model results in an already considerable height loss for the lowest acceleration. In Figure 24, the takeoff at a skid height of $H_{SKID}=2m$ is just performable without ground contact for the low acceleration $\dot{u}_{Kg}=1m/s^2$. More critical is the takeoff at a skid height of $H_{SKID}=1m$, Figure 25, where the acceleration of $\dot{u}_{Kg}=1m/s^2$ results in a ground contact. Simulation investigations have shown that, for this skid height, also lower accelerations down to $\dot{u}_{Kg}=0.1m/s^2$ result in a height loss greater than 1m. It is known from BO 105 flight tests, that a takeoff with constant power at a height of $H_{SKID}=1m$ is performable without ground contact, assuming a careful acceleration. However the increase of power required with forward velocity given by the modified source model agrees well with the flight test data for stationary flight states, see Figures 11 and 12. Figure 19 has shown the significant influence of accelerations on the increase of power factor. This has been explained by the time lag or the time delay associated with the development of the recirculation. Taking this effect into account for the factor X_{GV}, a simple filter of first order is used, a simple differential equation of first order, respectively:

$$X_{GV,O} + T_L \cdot \dot{X}_{GV,O} = X_{GV,I} \qquad (23)$$

where $X_{GV,I}$ is the input of the filter.

The results from the simulation with the modified source model, including a time lag, are shown in Figure 26 for two skid heights and different time constants. The horizontal acceleration is $\dot{u}_{Kg}=1m/s^2$. A time constant of $T_L=0.1s$ has nearly no effect on the height loss and can be regarded as stationary ground effect, i.e. ground effect from the modified source model without time lag. The height loss for both skid heights is considerably reduced with increasing time lag. The takeoff at a skid height of $H_{SKID}=1m$ is now possible without ground contact for a time constant of $T_L=10s$. This seems to be a relatively high time lag and further takeoff simulations have been carried out for different horizontal accelerations.

Figure 27 shows the height loss as a function of horizontal acceleration and time constant for two skid heights. The less critical case of a takeoff at skid height $H_{SKID}=2m$ is shown in the lower figure. The time constant has a significant influence on the height loss. Note, that for time constants of $T_L=5s$ and $T_L=10s$ a minimum height loss occurs for low horizontal acceleration. The takeoff at a skid height of $H_{SKID}=1m$ can be performed without ground contact, assuming a time constant in the order of $T_L=5s$ and larger.

Figure 28 shows the influence of horizontal acceleration and time lag on the power factor for a non-dimensional height $\bar{H}$=0.68, which is comparable to Figure 19. The power factor in this figure does not include acceleration power. In contrast to Figure 19, where the momentum theory is used for comparison, here, the performance calculation with the modified source model including a time lag is shown. A non-dimensional time lag of $\bar{T}_L$=10.4 gives similar reduction of the recirculation influence with increasing non-dimensional accelerations in comparison to Figure 19.

Flight tests to investigate takeoff with and without power excess have been carried out with the helicopter BO 105 of the DFVLR. Figure 29 shows height and power required from flight test and simulation versus time. The takeoff with a helicopter mass of m=2100kg is performed with nearly constant power, whereas the takeoff with m=2250kg is performed with low power excess. Unfortunately, the pilot did not hold constant collective pitch, thus small variations in power occur. As boundary condition for the comparison, the flight path from flight test, the longitudinal velocities and accelerations, respectively, are predetermined for the simulation. In both cases the theoretical power required from the simulation agrees well with the experimental power required from flight test. For the takeoff with nearly constant power, a considerable height loss can be seen from the figure. The takeoff with higher helicopter mass and low excess power is performed nearly without height loss. Figure 30 shows the flight path and power required versus takeoff distance. The difference between the takeoff distances, reaching a height of H=15m, is about 40m. The flight path angle is nearly the same. Note, that in the case of low power excess (m=2250kg) the height of H=15m is reached about 10s earlier. This is explained by higher horizontal accelerations at the beginning of takeoff.

The ground effect is of primary interest for takeoff, though the landing also is influenced by the ground effect. This can be clearly shown for the vertical landing, where the influence of horizontal velocity on power required is excluded. For a vertical landing with constant power, Figure 31 shows vertical velocity and height versus time. The landing starts with a vertical velocity of w_{Kg}=1.0m/s at a height of H≈30m. The landing is performed with a power setting, required for stationary descent. The data field simulation with the source model gives a continuous deceleration with decreasing height due to the ground cushion effect. At a height of H≈4m the stationary hover is reached. The oscillations in vertical velocity are small and the minimum height is close to the stationary hover height. In addition, the result from data field simulation with a source model, modified for hover, is shown. For the modification a polynomial has been used, which agrees well with the experimental ground effect data for hover, see Figure 5. It is assumed that the stationary ground effect also is valid for low descent velocities. Note the increasing rate of descent at a certain height, where the maximum power required IGE occurs for stationary hover.The oscillations in vertical velocity are considerable greater and the minimum height is about half of the stationary hover height. Higher descent velocities, lower power settings, respectively, are critical, since ground contact may be unavoidable.

6. Concluding Remarks

The influence of steady state ground effect on power required in hover and forward flight has been shown by means of flight test for the helicopter BO 105. The flight test data have been compared with theoretical results from performance calculations. The performance calculation contains a modified source model. A semi-empirical approach, which can be adjusted to match flight test data, is used to modify the source model, thus the theoretical results agree well with the experimental results. The calculation of power required with high accuracy for flight states IGE as well as OGE is required for the simulation of takeoff and landing procedures.

In addition, the influence of steady state and dynamic ground effect on power required in forward flight has been shown by means of model rotor test data. Although the model test data are not quantitatively comparable to the flight tests, important statements can be taken from these tests. In forward flight IGE at low forward velocities two distinct flow regions, the recirculation and the ground vortex region, exist. For low velocities a great recirculation pattern forms in front of the rotor. The recirculation is responsible for the increase of the induced velocity at the leading edge of the rotor, and thus the increase of power required for constant thrust. With increasing velocity the recirculation diminishes and a well defined ground vortex arises under the rotor. This ground vortex induces an upflow at the leading edge of the rotor, thus power required decreases. The ground vortex moves backwards with increasing velocity until it disappears behind the rotor.

A further important result of the model rotor tests is the sensitivity of ground effect to horizontal acceleration and deceleration, indicating that significant time constants are associated with the development of these flow fields. Low accelerations delay the build up of recirculation in such a way that the inflow occurs at a correspondingly higher velocity, while at high accelerations there is insufficient time for the recirculation to be set up. The non-dimensional time constant is in the order of $\bar{T}_L$=10. For accelerated forward flight states IGE, the strong increase of power required, which is characteristic of steady state ground effect, is not reached.

The dynamic ground effect has been taken into account by including a time delay of first order described by a differential equation of first order in the data field simulation. It has been shown by means of simulation results, that the time constant has an important influence on the height loss associated with takeoff without power excess, thus the dynamic ground effect is not neglectable. Also these results indicate that a time constant in the order of $\bar{T}_L$=10 gives height loss that agrees with flight test. The comparison of power required from simulation with power required from BO 105 flight test shows good agreement for takeoff without and with low power excess.

The vertical landing with constant power setting has been discussed by means of simulation results. With the assumption that stationary ground effect in hover also is valid for low vertical descent velocities, a considerable vertical acceleration is obtained at certain heights, where power required IGE increases exceeding power required OGE. In contrast to classical ground effect theory, BO 105 flight test data IGE show a maximum power required for heights in the order of $\bar{H}$=2.5 . This may be explained by an outer recirculation in hover comparable to the inner recirculation at the rotor center. However, no flow visualization studies are known, which indicate an outer recirculation is present in hover.

7. References

/1/ H.G. KÜSSNER, Probleme des Hubschraubers, Jahrbuch der deutschen Luftfahrtforschung, 1937

/2/ A. BETZ, Die Hubschrauber in Bodennähe, Jahrbuch der deutschen Luftfahrtforschung, 1937

/3/ M. KNIGHT, R.A. HEFNER, Analysis of Ground Effect on the Lifting Airscrew, NACA TN-835, 1941

/4/ I.C. CHEESEMAN, N.E. BENNETT, The Effect of the Ground on a Helicopter Rotor in Forward Flight, AAEE Report, Rep. and Mem. No. 3021, 1955

/5/ H.H. HEYSON, Ground Effect for Lifting Rotors in Forward Flight, NASA TN D-234, 1960

/6/ M. SUN, A Study of Helicopter Rotor Aerodynamics in Ground Effect at Low Speed, Ph.D. Thesis, Dept. of Mech. and Aerosp. Eng., Princeton University, 1983

/7/ J.S. HAYDEN, The Effect of the Ground on Helicopter Hovering Power Required, 32nd AHS (American Helicopter Society) Forum, 1976

/8/ K. LIESE, J. RUSSOW, G. REICHERT, Correlation of Generalized Helicopter Flight Test Performance Data with Theory, 13th ERF (European Rotorcraft Forum), 1987

/9/ H.H. HEYSON, Theoretical Study of the Effect of Ground Proximity on the Induced Efficiency of Helicopter Rotors, NASA TM X-71951, 1977

/10/ T. CERBE, J. RUSSOW, M. PLEHN, V. SCHARP, Durchführung und Auswertung von Hubschrauberflugversuchen, Interner Bericht 87-1, Institut für Flugmechanik, Technische Universität Braunschweig, 1987 (unpublished)

/11/ H.G. KÜSSNER, Untersuchung des Bodeneinflusses bei Hubschraubern, AVA-Bericht B 44/J/8, 1944

/12/ M.E. JACKSON, R.L. HOUSE, Exhaust Gas Reingestion During Hover in Ground Effect, 37th AHS Forum, 1981

/13/ R.J. HUSTON, C.E.K. MORRIS Jr., A Wind-Tunnel Investigation of Helicopter Directional Control in Rearward Flight in Ground Effect, NASA TN D-6118, 1971

/14/ R.W. EMPEY, R.A. ORMISTON, Tail Rotor Thrust on a 5.5-foot Helicopter Model in Ground Effect, 30th AHS Forum, 1974

/15/ P.F. SHERIDAN, W. WIESNER, Aerodynamics of Helicopter Flight near the Ground, 33rd AHS Forum, 1977

/16/ H.H. HEYSON, Operational Implications of some NACA/NASA Rotary Wing Induced Velocity Studies, NASA TM-80232, 1980

/17/ H.C. CURTISS Jr., M. SUN, W.F. PUTMAN, E.J. HANKER, Rotor Aerodynamics in Ground Effect at Low Advance Ratios, 37th AHS Forum, 1981

/18/ CHENJIAN HE, ZHENG GAO, A Study of the Rotor Wake in NOE, Seminar "The Theoretical Basis of Helicopter Technology", Nanjing, Pap.No. A-1, Nov. 1985

/19/ T. CERBE, G. REICHERT, Simulation Models for Optimization of Helicopter Takeoff and Landing, 13th ERF, 1987

/20/ H.C. CURTISS Jr., W. ERDMAN, M. SUN, Ground Effect Aerodynamics, Vertica, Vol. 11, No. 1/2, 1987

/21/ H.C. CURTISS Jr., M. SUN, W.F. PUTMAN, E.J. HANKER, Rotor Aerodynamics in Ground Effect at Low Advance Ratios, Journal of the American Helicopter Society, 29, 1984

/22/ H.C. CURTISS Jr., W.F. PUTMAN, E.J. HANKER, Rotor Aerodynamics in Ground Effect at Low Advance Ratios, Princeton University MAE Report No. 1571, July 1982

/23/ W. ERDMAN, Investigating Inflow Model Refinements for Hingeless Rotor Helicopters in Ground Effect, M.S.E. Thesis, Princeton University, MAE Department, no. 1752-T, 1986

/24/ P.F. SHERIDAN et al., Math Modeling for Helicopter Simulation of Low Speed, Low Altitude and Steeply Descending Flight, NASA CR 166385, July 1982

/25/ T. CERBE, G. REICHERT, Optimization of Helicopter Takeoff and Landing, 16th ICAS (International Council of the Aeronautical Sciences) Congress, 1988

Acknowledgements - The research at the Technical University of Braunschweig was supported by the DFG under SFB 212 "Sicherheit im Luftverkehr"

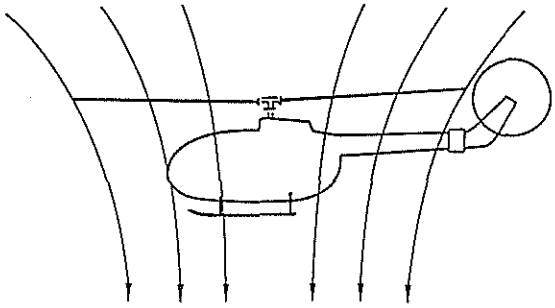

Figure 1 Helicopter Hovering OGE

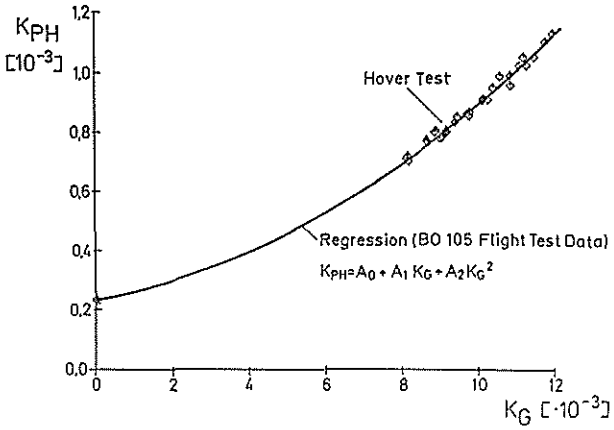

Figure 4 Power Coefficient in Hover OGE

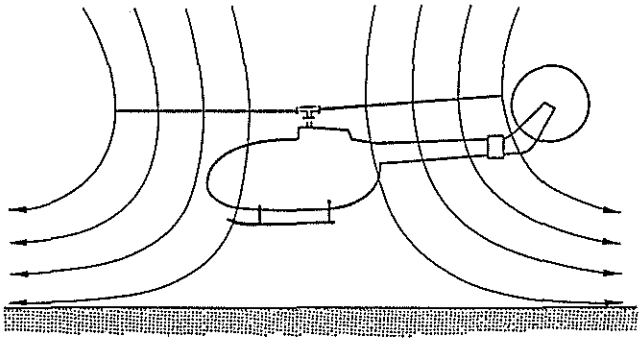

Figure 2 Helicopter Hovering IGE

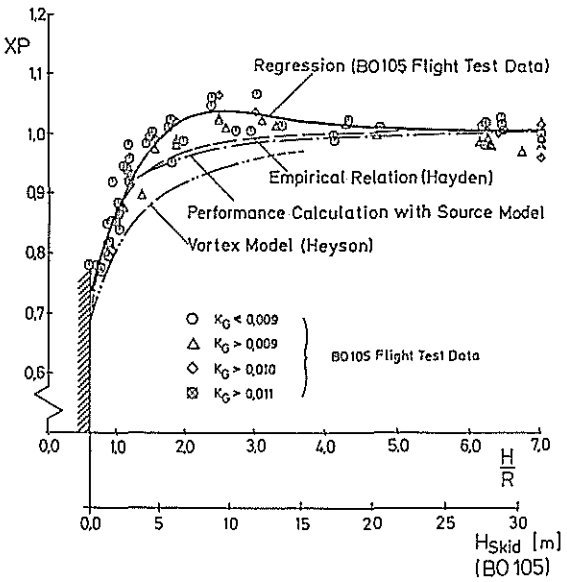

Figure 5 Power Factor in Hover IGE

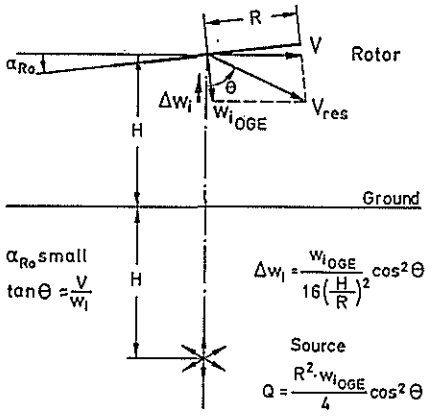

Figure 3 Source Model for Forward Flight IGE

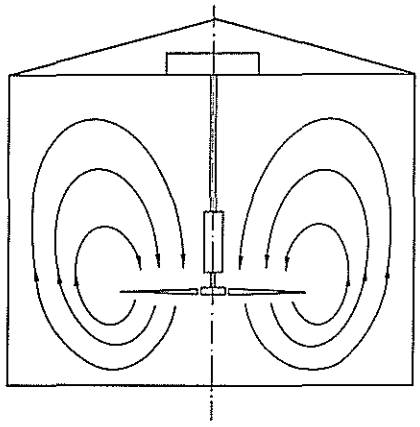

Figure 6 Recirculation for Model Rotor Testing in Closed Rooms

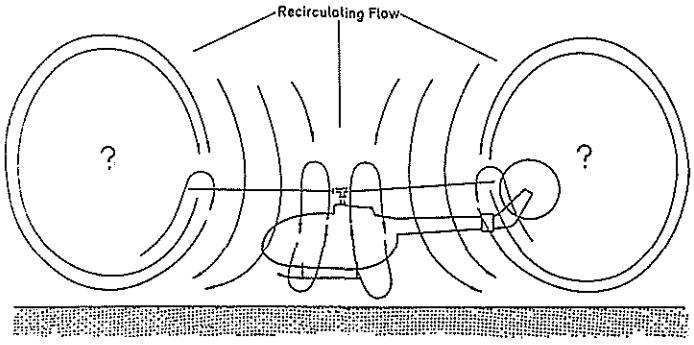

Figure 7 Recirculating Flow for Helicopter Hovering IGE

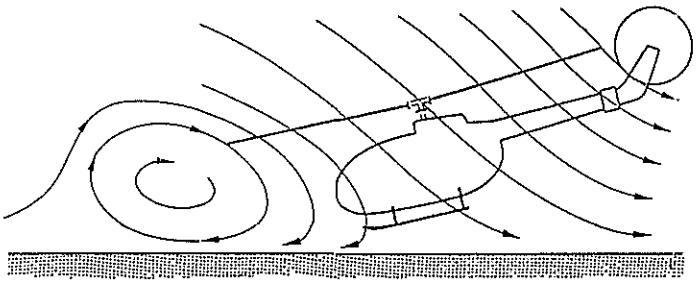

Figure 8 Recirculation in Forward Flight IGE

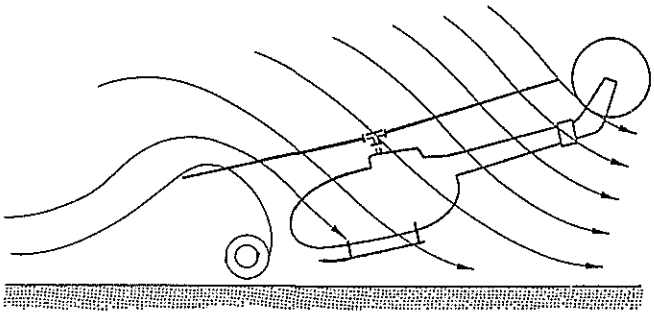

Figure 9 Ground Vortex in Forward Flight IGE

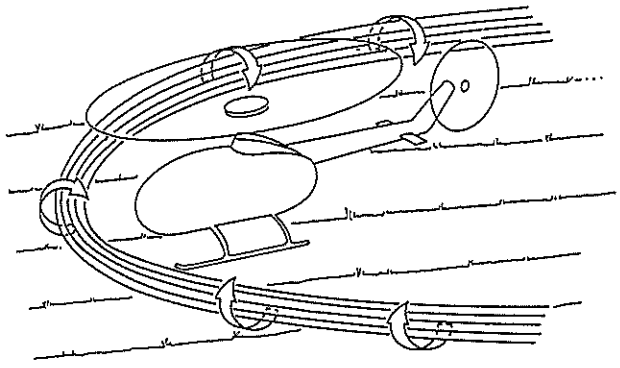

Figure 10 Horseshoe Vortex Pattern in Forward Flight IGE

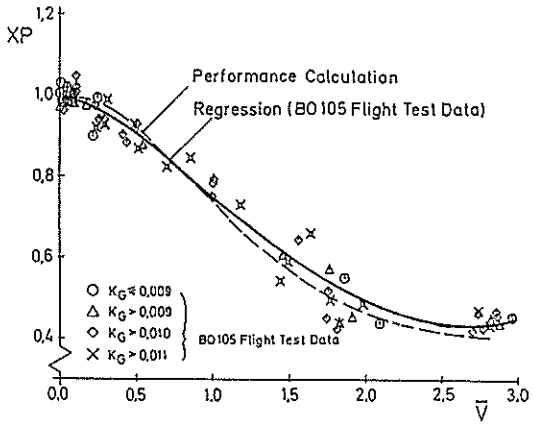

Figure 11 Power Factor in Forward Flight OGE

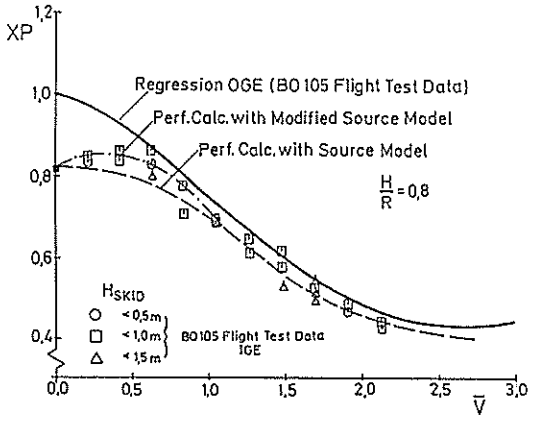

Figure 12 Power Factor in Forward Flight IGE

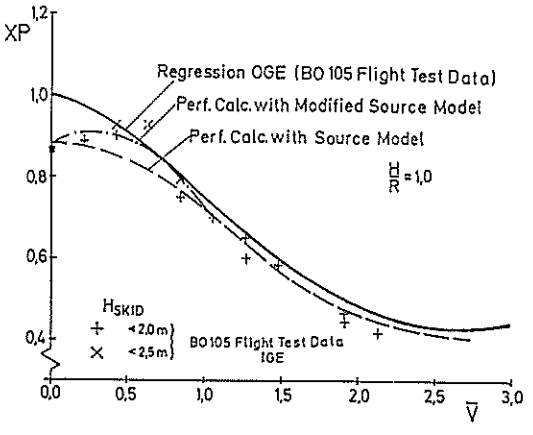

Figure 13 Power Factor in Forward Flight IGE

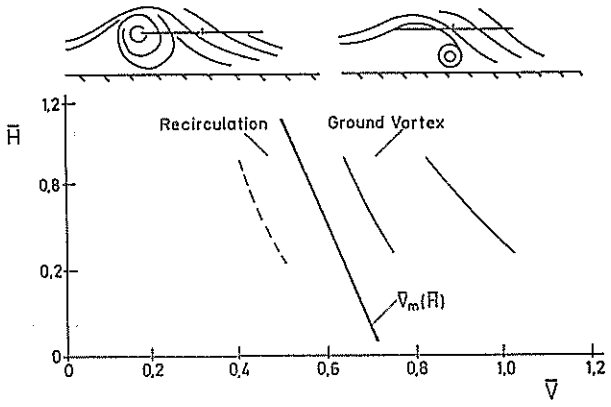

Figure 14 Recirculation and Ground Vortex Regions

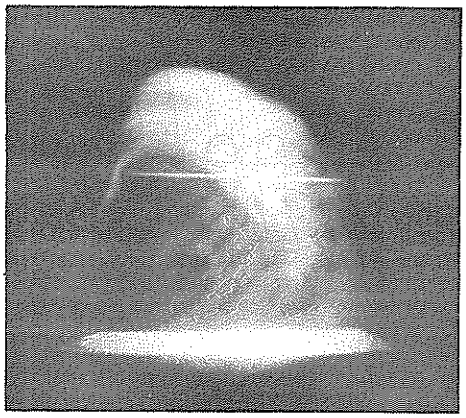

Figure 17 Ground Vortex State from Flow Visualization Studies

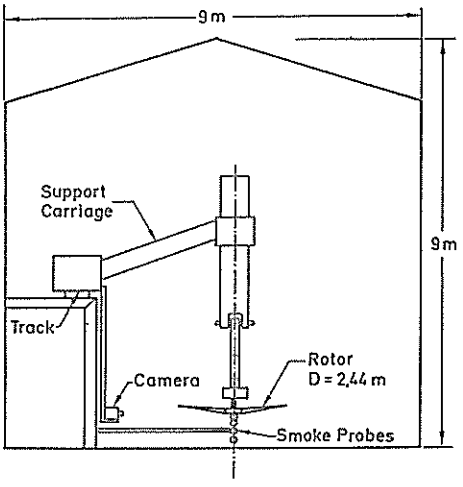

Figure 15 Cross Section of Test Facility at Princeton University

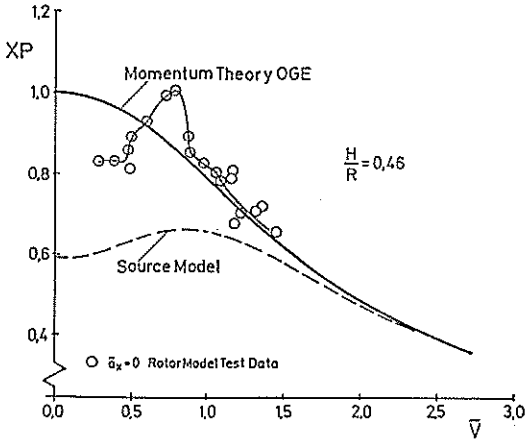

Figure 18 Power Factor in Forward Flight IGE Stationary Ground Effect

Figure 16 Recirculation State from Flow Visualization Studies

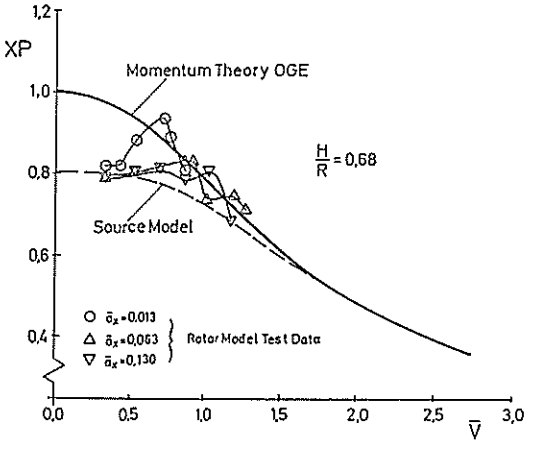

Figure 19 Power Factor in Forward Flight IGE Influence of Acceleration

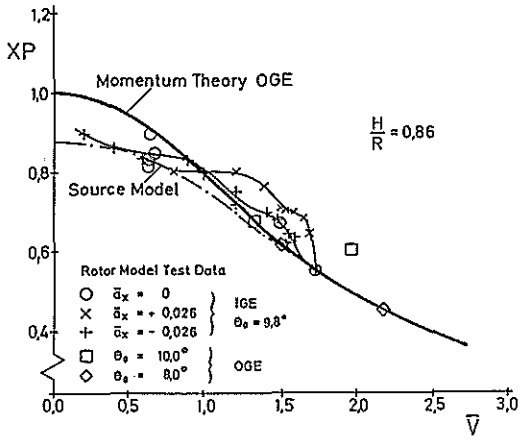

Figure 20 Power Factor in Forward Flight IGE Influence of Acceleration/Deceleration

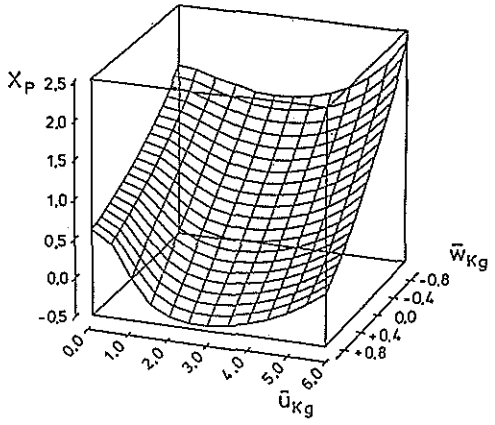

Figure 21 Power Factor in Forward Flight with Climb and Descent

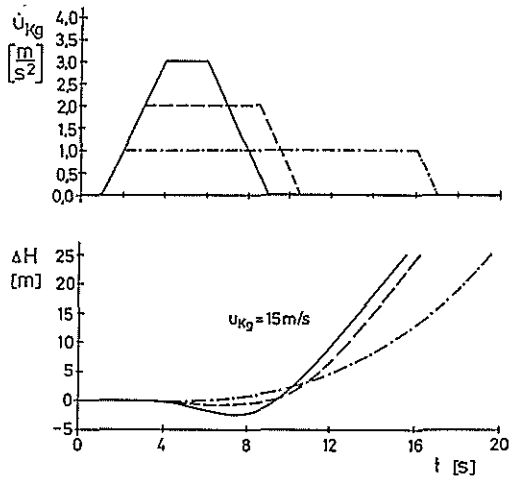

Figure 22 Takeoff with Constant Hover Power OGE Influence of Acceleration

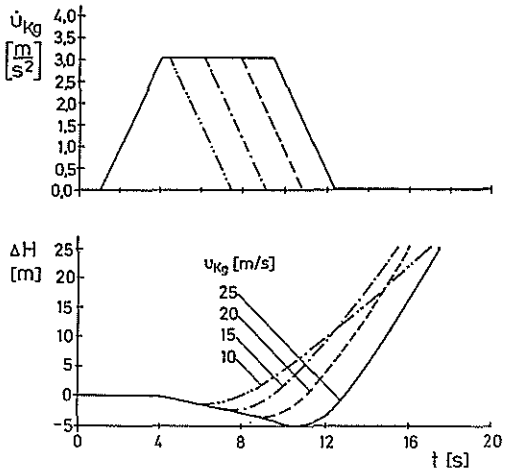

Figure 23 Takeoff with Constant Hover Power OGE Influence of Velocity

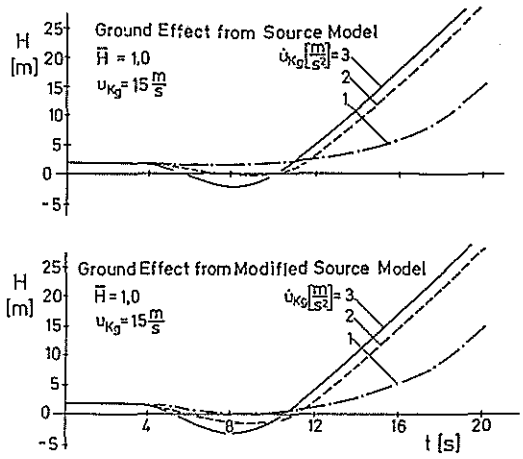

Figure 24 Takeoff with Constant Hover Power IGE Influence of Acceleration

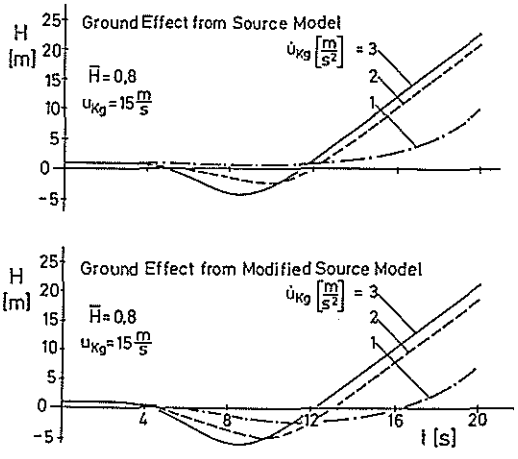

Figure 25 Takeoff with Constant Hover Power IGE Influence of Acceleration

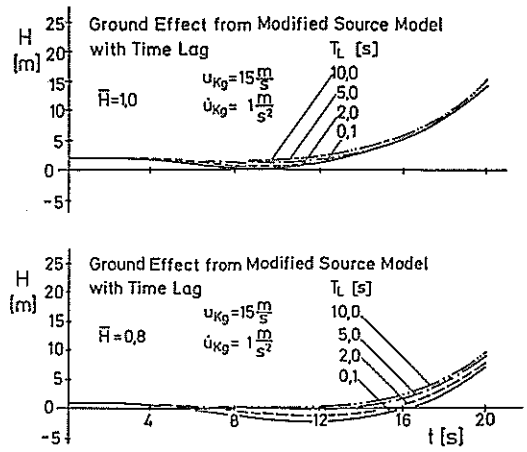

Figure 26 Takeoff with Constant Hover Power IGE Influence of Time Lag

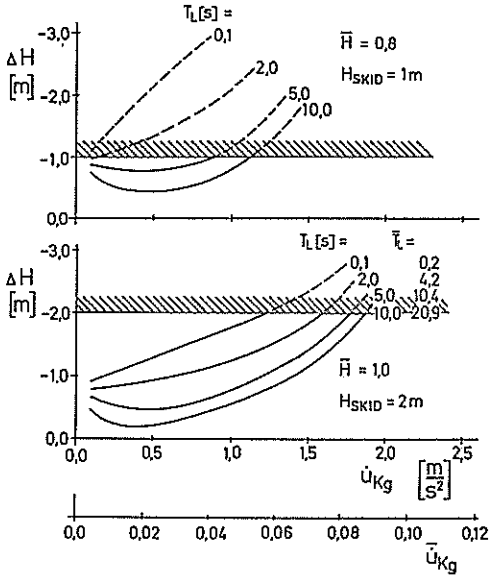

Figure 27 Takeoff with Constant Hover Power IGE Influence of Acceleration and Time Lag

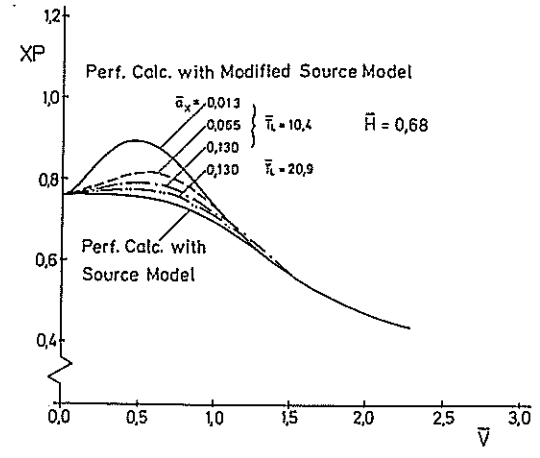

Figure 28 Power Factor in Forward Flight IGE Influence of Acceleration and Time Lag

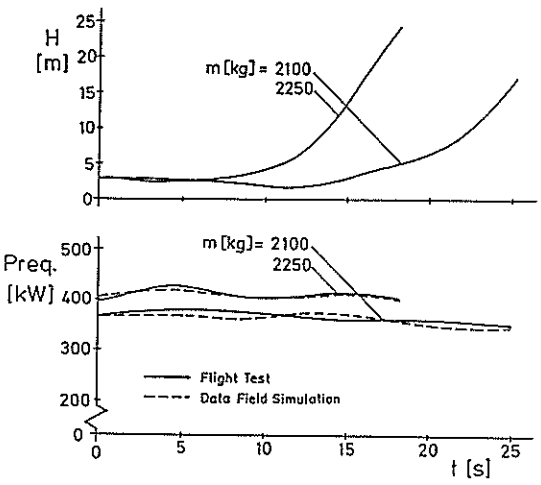

Figure 29 Takeoff with Low Power Excess

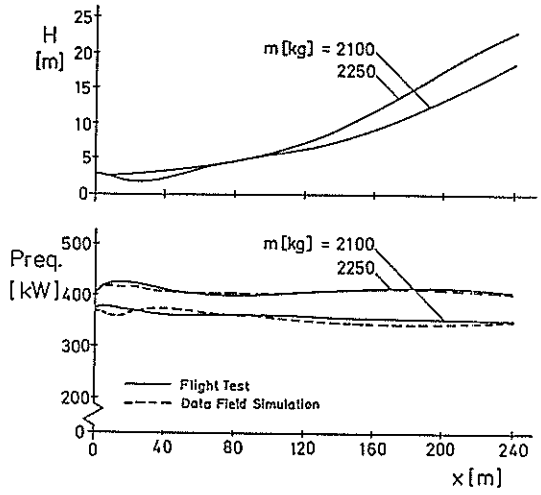

Figure 30 Takeoff with Low Power Excess

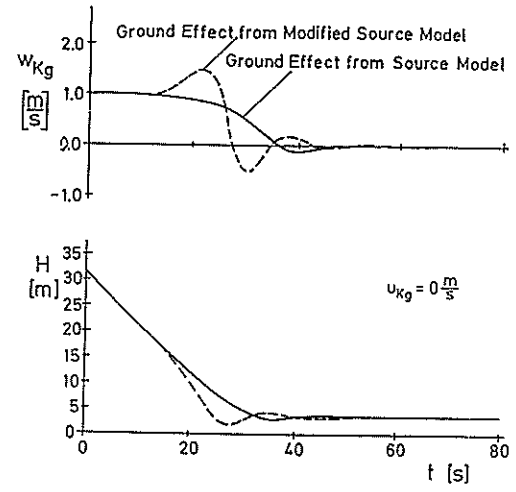

Figure 31 Vertical Landing with Constant Power for Descent